Two Power Allocation and Beamforming Strategies for Active IRS-aided Wireless Network via Machine Learning

Qiankun CHENG [1], Jiatong BAI [1], Xuehui WANG [1], Baihua SHI [1,2], Wei GAO [1], Feng SHU [1,2]

[1] School of Information and Communication Engineering, Hainan University, Haikou 570228, China
[2] School of Electronic and Optical Engineering, Nanjing University of Science and Technology, Nanjing 210094, China

cqk1129@hainanu.edu.cn, 18419229733@163.com, wangxuehui0503@163.com,
shibh56h@foxmail.com, gaowei@hainanu.edu.cn, shufeng0101@163.com

Abstract. *In this paper, a system utilizing an active intelligent reflecting surface (IRS) to enhance the performance of wireless communication network is modeled, which has the ability to adjust power between base station (BS) and active IRS. We aim to maximize the signal-to-noise ratio (SNR) of the user by jointly designing power allocation (PA) factor, active IRS phase shift matrix, and beamforming vector of BS, subject to a total power constraint. To tackle this non-convex problem, we solve this problem by alternately optimizing these variables. The PA factor is designed via polynomial regression method in machine learning. BS beamforming vector and IRS phase shift matrix are obtained by Dinkelbach's transform and successive convex approximation methods. Then, we maximize achievable rate (AR) and use closed-form fractional programming (CFFP) method to transform the original problem into an equivalent form. This problem is addressed by iteratively optimizing auxiliary variables, BS and IRS beamformings. Thus, two iterative PA methods are proposed accordingly, namely maximizing SNR based on PA factor (Max-SNR-PA) and maximizing AR based on CFFP (Max-AR-CFFP). The former has a better rate performance, while the latter has a lower computational complexity. Simulation results show that the proposed algorithms can effectively improve the rate performance compared to fixed PA strategies, only optimizing PA factor, aided by passive IRS, and without IRS.*

Keywords

Active intelligent reflecting surface, achievable rate, power allocation, closed-form fractional programming

1. Introduction

With the rapid development of 5th generation communication technology and the emergence of a large number of new applications such as augmented reality and virtual reality, the demand for high quality and high speed wireless communication network is growing day by day [1–4]. However, high-rate wireless networks also face some new challenges, like high costs and high energy consumption. The realization of green wireless transmission has become the consensus of industry and academia [5–7]. As a low-cost, low-power reflector, intelligent reflecting surface (IRS) provides a new way for future green wireless communication [8–10].

In an IRS-aided multiple-input single-output (MISO) system [11], two optimization schemes were proposed to minimize the power consumption at base station (BS) by jointly optimizing the transmitting beamforming of BS and phase shift matrix of IRS, given the signal-to-noise (SNR) target of the receiving end user. In [12], by using a deep reinforcement learning neural network, it was possible to simultaneously optimize transmit beamforming at BS and phase shift matrices at IRS to maximize ergodic sum rate in an IRS-aided multiuser downlink MISO system. In [13], the authors introduced IRS into secure multiple-input multiple-output (MIMO) wireless powered communication networks. A secrecy rate maximization problem was investigated and alternating optimization methods were constructed based on mean-square error and dual subgradient techniques to solve this non-convex problem. Literature [14] studied an IRS-assisted MIMO system, by iteratively optimizing the precoding beamformings in every BSs and phase shift beamforming in IRS, block coordinate descent and complex circle manifold methods are proposed to maximize the weighted sum rate. The deployment of IRS can significantly improve the performance of cell edge users compared to MIMO communication systems without IRS.

Although the power consumption of passive IRS mainly composed of passive reflective elements is significantly lower than that of active IRS, recent studies have shown that active IRS may have superiorities in some scenarios [15–18]. The power gain achieved by passive IRS is limited in some cases due to the fact that double fading effect caused by signal transmission over the BS-to-IRS and IRS-to-user channels [19]. By using active IRS with power amplifiers, the impact of double fading can be reduced [20]. The authors in [21] compared the performance of active and passive IRS-assisted

communication systems with the same total power budget, which proved that active IRS was superior to passive IRS when the power budget and the number of IRS elements are at a moderate level. The achievable rate (AR) maximization problem was studied in [22] in an active IRS-aided single-input single-output system, closed-form maximum ratio reflecting and selective ratio reflecting methods were proposed to optimize IRS precodings. Zhu et al. [23] investigated the sum-rate maximization problem in an active IRS-assisted multi-user MISO system, which the iterative optimization approach was developed based on second-order cone programming and majorization-minimization methods. Based on the above analysis, active IRS has more advanced features than passive IRS. To further improve the performance of communication system, we introduce active IRS and design active IRS and BS as an integrated system for joint control. In this case, it is natural to assume that active IRS will share a power supply with BS, and the optimal AR can be obtained by rationally distributing the power of BS and active IRS. Also this assumption facilitates performance comparisons with other systems.

The power allocation (PA) strategy can further improve rate performance under the condition that total power consumption of communication system is limited, which has been researched in [24–27]. Specifically, a secrecy rate (SR) maximization problem was established and a PA strategy was proposed in a secure directional modulation system after specifying secrecy symbol and artificial noise beamformings [28]. The maximum SR of a secure spatial modulation system was investigated in [29] and two PA strategies were provided based on gradient descent method. The authors in [30] studied the total power consumption minimization problem in a cooperative downlink multi-user system and proposed a scheme for joint optimization of spectrum and PA factors. Two iterative algorithms, including inter-node and intra-node PA phases, were proposed for a full-duplex decode-and-forward MIMO relay system to improve the rate performance of users end [31].

The aforementioned research primarily centers on power distribution in wireless networks without IRS. Compared to passive IRS and without IRS, active IRS can provide higher beamforming gain and also incur higher power consumption. Thus, upon incorporating active IRS into the communication system, we investigated the potential rate improvement achievable by dynamically allocating power between the BS and active IRS, in contrast to traditional fixed PA, passive IRS and without IRS. In this paper, our focus shifts to the development of two high-performance iterative PA strategies aimed at achieving corresponding PA gains. Our main contributions are outlined as follows:

- An active IRS-assisted PA wireless network system model is constructed and a PA strategy named Max-SNR-PA is proposed. We maximize SNR at user by jointly optimizing PA factor, BS transmit beamforming, and IRS phase shift matrix. Due to the fact that vari-

ables in objective function are coupled to each other, solving this problem directly is challenging. To deal with this difficulty, we adopt an alternate optimization approach. First, PA factor can be obtained by using polynomial regression method. Then, a successive convex approximation (SCA) technique in [32] is used to get BS transmit vector. Finally, a suboptimal iterative algorithm based on Dinkelbach's transform is applied for optimizing IRS phase shift beamforming.

- To reduce the computational complexity of the Max-SNR-PA strategy, a low-complexity Max-AR-CFFP algorithm is proposed. Here, we reformulate the system model with the goal of maximizing AR. Then, the objective function can be transformed into a equivalent form by using closed-form fractional programming (CFFP) method in [33], [34]. Next, we can use alternate iterative methods to obtain locally optimal solutions for BS and IRS beamformings. Simulation results show that: (a) the polynomial regression function can fit the original PA factor function well, (b) both of our proposed PA strategies can quickly achieve convergence, (c) compared with the case of fixed PA strategy in [35], gradient ascent (GA) method in [36], passive IRS, and without IRS, the two proposed PA strategies can effectively improve the rate performance.

The reminder of this paper is organized as follows. The system model with PA strategy is shown in Sec. 2. Two iterative PA algorithms are proposed in Sec. 3 and Sec. 4. Simulation results are presented in Sec. 5 and conclusions are drawn in Sec. 6.

Notations: During this paper, matrices and vectors are denoted as uppercase letters and lowercase letters, respectively. $\mathbb{C}$ represents a set of complex numbers. $(\cdot)^{\mathrm{H}}$, $(\cdot)^{\mathrm{T}}$, $(\cdot)^{*}$, $\| \cdot \|$, $\mathrm{diag}(\cdot)$, $E\{\cdot\}$, and $\Re\{\cdot\}$ denote the conjugate transpose, transpose, conjugate, Euclidean norm, diagonal, expectation and real part operations, respectively. $\mathbf{I}_N$ represents the $N \times N$ identity matrix.

2. System Model

2.1 System Model with PA Factor

As shown in Fig. 1, we consider an active IRS-assisted wireless network with PA. BS is equipped with M antennas. The user is equipped with a single antenna, and active IRS is equipped with N elements. The channel state information (CSI) of all links can be obtained by existing channel estimation technique [10]. Therefore, the CSI of all channels is assumed to be available at BS, active IRS, and user. $\mathbf{G} \in \mathbb{C}^{N \times M}$, $\mathbf{f}^{\mathrm{H}} \in \mathbb{C}^{1 \times N}$, and $\mathbf{h}^{\mathrm{H}} \in \mathbb{C}^{1 \times M}$ stand for the channels from BS to active IRS, active IRS to user, BS to user, respectively. The transmitted signal at BS is given by

$$\mathbf{s}_{\mathrm{B}} = \sqrt{\beta P_{\max}} \mathbf{v} x \qquad (1)$$
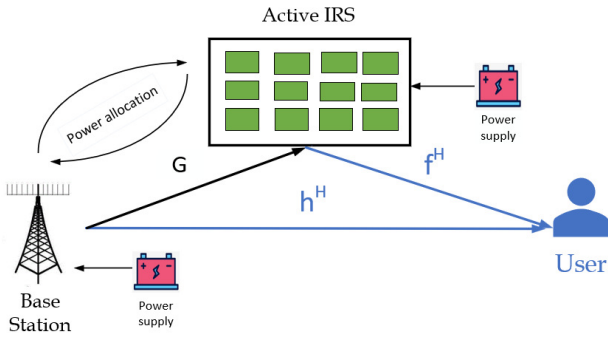
Fig. 1. System model of an active IRS-assisted wireless network with PA.

where $\mathbf{v} \in \mathbb{C}^{M \times 1}$ is the transmit beamforming of BS that meets the condition $\mathbf{v}^{\mathrm{H}}\mathbf{v} = 1$, $P_{\max}$ is the upper limit of the sum of power consumption by BS and active IRS, β is the PA factor within interval $[0, 1]$, and x denotes the transmit symbol satisfying $\mathbb{E}\left\{|x|^2\right\} = 1$.

For active IRS, let a_m and θ_m represent amplification coefficient of the m-th element and phase shift of m-th element respectively, where $m = 1, \cdots, N$. $\mathbf{\Theta} = \mathrm{diag}\left(a_1 \mathrm{e}^{\mathrm{j}\theta_1}, \cdots, a_N \mathrm{e}^{\mathrm{j}\theta_N}\right)$ denotes the reflective beamforming matrix of active IRS. The signal reflected by active IRS can be written as:

$$\mathbf{s}_{\mathrm{I}} = \mathbf{\Theta}\mathbf{G}\mathbf{s}_{\mathrm{B}} + \mathbf{\Theta}\mathbf{n}_{\mathrm{I}} = \sqrt{\beta P_{\max}}\mathbf{\Theta}\mathbf{G}\mathbf{v}x + \mathbf{\Theta}\mathbf{n}_{\mathrm{I}} \qquad (2)$$

where $\mathbf{n}_{\mathrm{I}} \in \mathbb{C}^{N \times 1}$ denotes the additive white Gaussian noise (AWGN) introduced by active IRS power amplifiers, $\mathbf{n}_{\mathrm{I}} \sim \mathcal{CN}\left(0, \sigma_{\mathrm{I}}^2\mathbf{I}_N\right)$.

The received signal at the user is given by

$$y = \sqrt{\beta P_{\max}}(\mathbf{f}^{\mathrm{H}}\mathbf{\Theta}\mathbf{G} + \mathbf{h}^{\mathrm{H}})\mathbf{v}x + \mathbf{f}^{\mathrm{H}}\mathbf{\Theta}\mathbf{n}_{\mathrm{I}} + z \qquad (3)$$

where z is the AWGN with distribution $z \sim \mathcal{CN}(0, \sigma_n^2)$.

The power consumed at active IRS can be expressed as

$$P_{\mathrm{IRS}} = E\{\mathbf{s}_{\mathrm{I}}^{\mathrm{H}}\mathbf{s}_{\mathrm{I}}\} = \beta P_{\max}||\mathbf{\Theta}\mathbf{G}\mathbf{v}||_2^2 + \sigma_{\mathrm{I}}^2||\mathbf{\Theta}||_{\mathrm{F}}^2. \qquad (4)$$

From (3), SNR at the user can be given by

$$\mathrm{SNR} = \frac{\beta P_{\max}||(\mathbf{f}^{\mathrm{H}}\mathbf{\Theta}\mathbf{G} + \mathbf{h}^{\mathrm{H}})\mathbf{v}||_2^2}{\sigma_{\mathrm{I}}^2||\mathbf{f}^{\mathrm{H}}\mathbf{\Theta}||_2^2 + \sigma_n^2}. \qquad (5)$$

The AR is

$$\mathrm{AR} = \log_2(1 + \mathrm{SNR}). \qquad (6)$$

2.2 System Model without PA Factor

In this subsection, let us consider the system model hides PA factor β.

The transmitted signal at BS is

$$\mathbf{s}_{\mathrm{B1}} = \mathbf{v}_1 x \qquad (7)$$

where $\mathbf{v}_1 \in \mathbb{C}^{M \times 1}$ is the transmit beamforming of BS.

The signal reflected by active IRS is:

$$\mathbf{s}_{\mathrm{I1}} = \mathbf{\Theta}\mathbf{G}\mathbf{s}_{\mathrm{B1}} + \mathbf{\Theta}\mathbf{n}_{\mathrm{I}} = \mathbf{\Theta}\mathbf{G}\mathbf{v}_1 x + \mathbf{\Theta}\mathbf{n}_{\mathrm{I}}. \qquad (8)$$

The received signal at the user can be given by

$$y_1 = (\mathbf{f}^{\mathrm{H}}\mathbf{\Theta}\mathbf{G} + \mathbf{h}^{\mathrm{H}})\mathbf{v}_1 x + \mathbf{f}^{\mathrm{H}}\mathbf{\Theta}\mathbf{n}_{\mathrm{I}} + z. \qquad (9)$$

The power consumed at BS and active IRS can be expressed as

$$\begin{aligned} P_{\mathrm{BS1}} &= \mathbf{v}_1^{\mathrm{H}}\mathbf{v}_1, \\ P_{\mathrm{IRS1}} &= ||\mathbf{\Theta}\mathbf{G}\mathbf{v}_1||_2^2 + \sigma_{\mathrm{I}}^2||\mathbf{\Theta}||_{\mathrm{F}}^2. \end{aligned} \qquad (10)$$

The SNR_1 is

$$\mathrm{SNR}_1 = \frac{||(\mathbf{f}^{\mathrm{H}}\mathbf{\Theta}\mathbf{G} + \mathbf{h}^{\mathrm{H}})\mathbf{v}_1||_2^2}{\sigma_{\mathrm{I}}^2||\mathbf{f}^{\mathrm{H}}\mathbf{\Theta}||_2^2 + \sigma_n^2}. \qquad (11)$$

The AR_1 can be written as

$$\mathrm{AR}_1 = \log_2(1 + \mathrm{SNR}_1). \qquad (12)$$

Equations (6) and (12) are just two different expressions of AR, and there is no essential difference between them. It has no effect on AR. The purpose of writing two forms with and without PA factor is to adopt different methods to solve the proposed optimization problem in next sections.

3. Proposed Max-SNR-PA Strategy

In this section, considering the system model with PA factor β, we maximize SNR by jointly optimizing PA factor β, active IRS phase shift matrix $\mathbf{\Theta}$, and BS beamforming vector $\mathbf{v}$. The overall optimization problem is formulated as:

$$\begin{aligned} (\mathrm{P0}) : \max_{\beta, \mathbf{\Theta}, \mathbf{v}} \quad & \mathrm{SNR} = \frac{\beta P_{\max}||(\mathbf{f}^{\mathrm{H}}\mathbf{\Theta}\mathbf{G} + \mathbf{h}^{\mathrm{H}})\mathbf{v}||_2^2}{\sigma_{\mathrm{I}}^2||\mathbf{f}^{\mathrm{H}}\mathbf{\Theta}||_2^2 + \sigma_n^2} \\ \mathrm{s.t.} \quad & 0 \leq \beta \leq 1, \ \mathbf{v}^{\mathrm{H}}\mathbf{v} = 1, \\ & \beta P_{\max}||\mathbf{\Theta}\mathbf{G}\mathbf{v}||_2^2 + \sigma_{\mathrm{I}}^2||\mathbf{\Theta}||_{\mathrm{F}}^2 \leq (1 - \beta)P_{\max}. \end{aligned}$$
$$(13)$$

Due to the coupled β, $\mathbf{\Theta}$, and $\mathbf{v}$, this optimization problem is difficult to solve. In general, there is no efficient method to solve problem (P0) directly. Therefore, in the following, we apply the alternating optimization algorithm and optimize β, $\mathbf{\Theta}$, and $\mathbf{v}$ alternately.

3.1 Optimize β by fixing $\mathbf{\Theta}$ and $\mathbf{v}$

Letting $\mathbf{\theta} = (a_1 \mathrm{e}^{\mathrm{j}\theta_1}, \cdots, a_N \mathrm{e}^{\mathrm{j}\theta_N})^{\mathrm{H}}$, the received signal at the user can be rewritten as

$$\begin{aligned} y = &\sqrt{\beta P_{\max}}(\rho \widetilde{\mathbf{\theta}}^{\mathrm{H}} \mathrm{diag}(\mathbf{f}^{\mathrm{H}})\mathbf{G} + \mathbf{h}^{\mathrm{H}})\mathbf{v}x \\ &+ \rho \widetilde{\mathbf{\theta}}^{\mathrm{H}} \mathrm{diag}(\mathbf{f}^{\mathrm{H}})\mathbf{n}_{\mathrm{I}} + z \end{aligned} \qquad (14)$$

where

$$\boldsymbol{\theta} = \rho\widetilde{\boldsymbol{\theta}}, \quad \rho = \|\boldsymbol{\theta}\|_2, \quad \|\widetilde{\boldsymbol{\theta}}\|_2 = 1. \tag{15}$$

The power consumed at active IRS is

$$P_{\text{IRS}} = \beta P_{\max}\rho^2\|\widetilde{\boldsymbol{\theta}}^{\text{H}}\operatorname{diag}(\mathbf{Gv})\|_2^2 + \sigma_{\text{I}}^2\rho^2. \tag{16}$$

In order to optimize β, we consider making the sum of consumed power of BS and active IRS reach the upper limit $P_{\max}$, which means that

$$P_{\text{IRS}} = (1-\beta)P_{\max}, \tag{17}$$

then we can obtain

$$\rho = \sqrt{\frac{(1-\beta)P_{\max}}{\beta P_{\max}\|\widetilde{\boldsymbol{\theta}}^{\text{H}}\operatorname{diag}(\mathbf{Gv})\|_2^2 + \sigma_{\text{I}}^2}}. \tag{18}$$

Thus, the SNR can be simplified as

$$\text{SNR} = \frac{\beta P_{\max}\|(\rho\widetilde{\boldsymbol{\theta}}^{\text{H}}\operatorname{diag}(\mathbf{f}^{\text{H}})\mathbf{G} + \mathbf{h}^{\text{H}})\mathbf{v}\|_2^2}{\sigma_{\text{I}}^2\rho^2\|\widetilde{\boldsymbol{\theta}}^{\text{H}}\operatorname{diag}(\mathbf{f}^{\text{H}})\|_2^2 + \sigma_n^2}. \tag{19}$$

Substituting (18) into (19) to simplify the optimization problem as

$$\begin{aligned}(\text{P1}) : \max_{\beta} \quad & f(\beta) = \frac{a\beta^2 + b\beta + 2c\beta\sqrt{d\beta^2 + e\beta + f}}{g\beta + h} \\ \text{s.t.} \quad & 0 \le \beta \le 1. \end{aligned} \tag{20}$$

where

$$\begin{aligned}a &= P_{\max}^2\|\mathbf{h}^{\text{H}}\mathbf{v}\|^2\|\widetilde{\boldsymbol{\theta}}^{\text{H}}\operatorname{diag}(\mathbf{Gv})\|^2 \\ &\qquad\qquad - P_{\max}^2\|\widetilde{\boldsymbol{\theta}}^{\text{H}}\operatorname{diag}(\mathbf{f}^{\text{H}})\mathbf{Gv}\|^2, \\ b &= P_{\max}^2\|\widetilde{\boldsymbol{\theta}}^{\text{H}}\operatorname{diag}(\mathbf{f}^{\text{H}})\mathbf{Gv}\|^2 + P_{\max}\|\mathbf{h}^{\text{H}}\mathbf{v}\|^2\sigma_{\text{I}}^2, \\ c &= P_{\max}\Re\{\widetilde{\boldsymbol{\theta}}^{\text{H}}\operatorname{diag}(\mathbf{f}^{\text{H}})\mathbf{Gvv}^{\text{H}}\mathbf{h}\}, \\ d &= -P_{\max}^2\|\widetilde{\boldsymbol{\theta}}^{\text{H}}\operatorname{diag}(\mathbf{Gv})\|^2, \\ e &= P_{\max}^2\|\widetilde{\boldsymbol{\theta}}^{\text{H}}\operatorname{diag}(\mathbf{Gv})\|^2 - \sigma_{\text{I}}^2 P_{\max}, \\ f &= P_{\max}\sigma_{\text{I}}^2, \\ g &= \sigma_n^2 P_{\max}\|\widetilde{\boldsymbol{\theta}}^{\text{H}}\operatorname{diag}(\mathbf{Gv})\|^2 - \sigma_{\text{I}}^2 P_{\max}\|\widetilde{\boldsymbol{\theta}}^{\text{H}}\operatorname{diag}(\mathbf{f}^{\text{H}})\|^2, \\ h &= \sigma_{\text{I}}^2 P_{\max}\|\widetilde{\boldsymbol{\theta}}^{\text{H}}\operatorname{diag}(\mathbf{f}^{\text{H}})\|^2 + \sigma_n^2\sigma_{\text{I}}^2. \end{aligned} \tag{21}$$

Due to the difficulty of directly solving the sub optimization problem (P1), in the following, we will use polynomial regression method in machine learning [37] to fit the objective function $f(\beta)$. Firstly, a Q-order polynomial $g(\beta)$ is constructed to approximate $f(\beta)$,

$$\begin{aligned}g(\beta) &= a_0 + a_1\beta + \cdots + a_Q\beta^Q \\ &= \left(1, \beta, \cdots, \beta^Q\right) \bullet \left(a_0, a_1, \cdots, a_Q\right)^{\text{T}}. \end{aligned} \tag{22}$$

To estimate the coefficients of the above polynomial, the training set S_{PR} is generated as

$$S_{\text{PR}} = \{(\beta_1, f(\beta_1)), (\beta_2, f(\beta_2)), \cdots, (\beta_J, f(\beta_J))\}. \tag{23}$$

Constructing the polynomial fitting matrix-vector form as follows:

$$\underbrace{\begin{pmatrix}g(\beta_1)\\ \vdots \\ g(\beta_J)\end{pmatrix}}_{\mathbf{g}} = \underbrace{\begin{pmatrix}1 & \beta_1 & \cdots & \beta_1^Q \\ \vdots & \vdots & \vdots & \vdots \\ 1 & \beta_J & \cdots & \beta_J^Q\end{pmatrix}}_{\mathbf{A}} \underbrace{\begin{pmatrix}a_0\\ \vdots \\ a_Q\end{pmatrix}}_{\mathbf{b}}, \tag{24}$$

$\mathbf{g} = \mathbf{Ab}$, where $J \ge 5(Q+1)$. Let us define the following target vector

$$\mathbf{c} = (f(\beta_1), \cdots, f(\beta_J))^{\text{T}}. \tag{25}$$

The corresponding square error summation is defined as

$$\begin{aligned}\Delta(\mathbf{b}) &= (\mathbf{g} - \mathbf{c})^{\text{T}}(\mathbf{g} - \mathbf{c})/J \\ &= \frac{1}{J}\left\{\mathbf{b}^{\text{T}}\mathbf{A}^{\text{T}}\mathbf{Ab} - \mathbf{c}^{\text{T}}\mathbf{Ab} - \mathbf{b}^{\text{T}}\mathbf{A}^{\text{T}}\mathbf{c} + \mathbf{c}^{\text{T}}\mathbf{c}\right\}. \end{aligned} \tag{26}$$

Taking the first derivative of $\Delta(\mathbf{b})$ with respect to $\mathbf{b}$ equal zero

$$\frac{\partial\Delta(\mathbf{b})}{\partial\mathbf{b}} = \frac{1}{J}\left\{2\mathbf{A}^{\text{T}}\mathbf{Ab} - 2\mathbf{A}^{\text{T}}\mathbf{c}\right\} = 0 \tag{27}$$

which yields

$$\hat{\mathbf{b}} = \left(\mathbf{A}^{\text{T}}\mathbf{A}\right)^{-1}\mathbf{A}^{\text{T}}\mathbf{c}. \tag{28}$$

We have completed the estimate of coefficients of polynomial $g(\beta)$ and obtained the fitting polynomial as follows:

$$\hat{g}(\beta) = \hat{a}_0 + \hat{a}_1\beta + \cdots + \hat{a}_Q\beta^Q. \tag{29}$$

Finding the stationary points of the above polynomial in interval $[0, 1]$ is equivalent to find the roots of the following polynomial:

$$\frac{\partial\hat{g}(\beta)}{\partial\beta} = Q\hat{a}_Q\beta^{Q-1} + \cdots + 2\hat{a}_2\beta + \hat{a}_1 = 0. \tag{30}$$

For example, when $Q = 2$, we have

$$2\hat{a}_2\beta + \hat{a}_1 = 0 \Rightarrow \bar{\beta} = \frac{-\hat{a}_1}{2\hat{a}_2}, \tag{31}$$

when $Q = 3$, we have

$$3\hat{a}_3\beta^2 + 2\hat{a}_2\beta + \hat{a}_1 = 0 \tag{32}$$

which yields

$$\bar{\beta}_1 = \frac{-\hat{a}_2 + \sqrt{\hat{a}_2^2 - 3\hat{a}_3\hat{a}_1}}{3\hat{a}_3}, \quad \bar{\beta}_2 = \frac{-\hat{a}_2 - \sqrt{\hat{a}_2^2 - 3\hat{a}_3\hat{a}_1}}{3\hat{a}_3}. \tag{33}$$

In order to guarantee that there are closed-form roots for the equation (30), the value of Q is taken to be an integer smaller than 6.

Considering $\beta \in [0, 1]$, we need to judge whether all candidate roots are within the interval $[0, 1]$, then we have

$$\widetilde{\beta}_i = \begin{cases} \bar{\beta}_i, \bar{\beta}_i \in [0, 1] \\ 0, \bar{\beta}_i \notin [0, 1] \end{cases} \tag{34}$$

where $i \in \{1, 2, \cdots, Q - 1\}$. The optimal solution of β is

$$\beta^o = \underset{\beta \in S_B}{\arg\max} \ f(\beta) \tag{35}$$

where set S_B is defined as

$$S_B = \left\{ 0, \widetilde{\beta}_1, \cdots, \widetilde{\beta}_{Q-1}, 1 \right\}. \tag{36}$$

3.2 Optimize v by Fixing β and Θ

In this subsection, beamforming vector of BS $\mathbf{v}$ is optimized by fixing PA factor β and active IRS phase shift matrix Θ. The optimization problem with respect to $\mathbf{v}$ is

$$(\text{P2}) : \max_{\mathbf{v}} \quad \text{SNR} = \frac{\beta P_{\max} ||(\mathbf{f}^H \Theta \mathbf{G} + \mathbf{h}^H) \mathbf{v}||_2^2}{\sigma_I^2 ||\mathbf{f}^H \Theta||_2^2 + \sigma_n^2}$$

$$\text{s.t.} \quad \mathbf{v}^H \mathbf{v} = 1,$$

$$\beta P_{\max} ||\Theta \mathbf{G} \mathbf{v}||_2^2 + \sigma_I^2 ||\Theta||_F^2 \le (1 - \beta) P_{\max}, \tag{37}$$

which can be re-arranged as

$$(\text{P2-1}) : \max_{\mathbf{v}} \quad \mathbf{v}^H \mathbf{B} \mathbf{v}$$

$$\text{s.t.} \quad \mathbf{v}^H \mathbf{v} = 1, \tag{38}$$

$$\mathbf{v}^H \mathbf{C} \mathbf{v} \le P'_{\max}$$

where

$$\begin{aligned} \mathbf{B} &= (\mathbf{f}^H \Theta \mathbf{G} + \mathbf{h}^H)^H (\mathbf{f}^H \Theta \mathbf{G} + \mathbf{h}^H), \\ \mathbf{C} &= \mathbf{G}^H \Theta^H \Theta \mathbf{G}, \\ P'_{\max} &= \frac{(1 - \beta) P_{\max} - \sigma_I^2 ||\Theta||_F^2}{\beta P_{\max}}. \end{aligned} \tag{39}$$

Due to the insensitivity of the objective function value to the scaling of $\mathbf{v}$, we relax the modulo constraint to $\mathbf{v}^H \mathbf{v} \le 1$, the optimization problem can be rewritten as

$$(\text{P2-2}) : \max_{\mathbf{v}} \quad \mathbf{v}^H \mathbf{B} \mathbf{v}$$

$$\text{s.t.} \quad \mathbf{v}^H \mathbf{v} \le 1, \tag{40}$$

$$\frac{\mathbf{v}^H \mathbf{C} \mathbf{v}}{\mathbf{v}^H \mathbf{v}} \le P'_{\max}.$$

However, the optimization problem (P2-2) is still non-convex. Therefore, we use SCA method in [32] to solve this problem. By referring to the first-order Taylor series expansion at fixed point $\tilde{\mathbf{v}}$, we have

$$\begin{aligned} \mathbf{v}^H \mathbf{B} \mathbf{v} &\ge 2\Re\{\tilde{\mathbf{v}}^H \mathbf{B} \mathbf{v}\} - \tilde{\mathbf{v}}^H \mathbf{B} \tilde{\mathbf{v}}, \\ \mathbf{v}^H \mathbf{v} &\ge 2\Re\{\tilde{\mathbf{v}}^H \mathbf{v}\} - \tilde{\mathbf{v}}^H \tilde{\mathbf{v}} \end{aligned} \tag{41}$$

then, the optimization problem is transformed into

$$(\text{P2-3}) : \max_{\mathbf{v}} \quad \Re\{\tilde{\mathbf{v}}^H \mathbf{B} \mathbf{v}\}$$

$$\text{s.t.} \quad \mathbf{v}^H \mathbf{v} \le 1, \tag{42}$$

$$\mathbf{v}^H \mathbf{C} \mathbf{v} \le P'_{\max} \left(2\Re\{\tilde{\mathbf{v}}^H \mathbf{v}\} - \tilde{\mathbf{v}}^H \tilde{\mathbf{v}} \right).$$

This is a convex optimization problem, and it can be solved by CVX. After obtain the solution $\bar{\mathbf{v}}$, the beamforming vector is designed as

$$\mathbf{v} = \frac{\bar{\mathbf{v}}}{|\bar{\mathbf{v}}|}. \tag{43}$$

3.3 Optimize Θ by Fixing β and v

In this subsection, we optimize Θ by fixing β and $\mathbf{v}$. Considering reflective beamforming vector θ, and on the basis of (3), the received signal at the user can be rewritten as

$$\begin{aligned} y &= \sqrt{\beta P_{\max}} (\theta^H \text{diag}(\mathbf{f}^H) \mathbf{G} + \mathbf{h}^H) \mathbf{v} x \\ &\quad + \theta^H \text{diag}(\mathbf{f}^H) \mathbf{n}_I + z, \end{aligned} \tag{44}$$

SNR is given by

$$\text{SNR} = \frac{\beta P_{\max} ||(\theta^H \text{diag}(\mathbf{f}^H) \mathbf{G} + \mathbf{h}^H) \mathbf{v}||_2^2}{\sigma_I^2 ||\theta^H \text{diag}(\mathbf{f}^H)||_2^2 + \sigma_n^2}. \tag{45}$$

The power consumed at active IRS can be reformulated as

$$\begin{aligned} P_{\text{IRS}} &= \beta P_{\max} ||\theta^H \text{diag}(\mathbf{G}\mathbf{v})||_2^2 + \sigma_I^2 \theta^H \theta \\ &= \beta P_{\max} \theta^H \text{diag}(\mathbf{G}\mathbf{v}) \text{diag}(\mathbf{G}\mathbf{v})^H \theta + \sigma_I^2 \theta^H \theta \\ &= \theta^H \left[\beta P_{\max} \text{diag}(\mathbf{G}\mathbf{v}) \text{diag}(\mathbf{G}\mathbf{v})^H + \sigma_I^2 \mathbf{I}_N \right] \theta. \end{aligned} \tag{46}$$

Simplifying the numerator and denominator terms in SNR can yield

$$\begin{aligned} &||(\theta^H \text{diag}(\mathbf{f}^H) \mathbf{G} + \mathbf{h}^H) \mathbf{v}||_2^2 \\ &= (\theta^H \text{diag}(\mathbf{f}^H) \mathbf{G} + \mathbf{h}^H) \mathbf{v} \mathbf{v}^H (\theta^H \text{diag}(\mathbf{f}^H) \mathbf{G} + \mathbf{h}^H)^H \\ &= (\theta^H \text{diag}(\mathbf{f}^H) \mathbf{G} + \mathbf{h}^H) \mathbf{v} \mathbf{v}^H (\mathbf{G}^H \text{diag}(\mathbf{f}^H)^H \theta + \mathbf{h}) \\ &= \theta^H \text{diag}(\mathbf{f}^H) \mathbf{G} \mathbf{v} \mathbf{v}^H \mathbf{G}^H \text{diag}(\mathbf{f}^H)^H \theta + \mathbf{h}^H \mathbf{v} \mathbf{v}^H \mathbf{h} \\ &\quad + 2\Re\{\mathbf{h}^H \mathbf{v} \mathbf{v}^H \mathbf{G}^H \text{diag}(\mathbf{f}^H)^H \theta\}, \\ &\sigma_I^2 ||\theta^H \text{diag}(\mathbf{f}^H)||_2^2 + \sigma_n^2 = \sigma_I^2 \theta^H \text{diag}(\mathbf{f}^H) \text{diag}(\mathbf{f}^H)^H \theta + \sigma_n^2. \end{aligned} \tag{47}$$

Thus, the optimization problem respect to θ can be recast as

$$(\text{P3}) : \max_{\theta} \quad \frac{\theta^H \mathbf{D} \theta + 2\Re\{\mathbf{t}^H \theta\}}{\theta^H \mathbf{E} \theta + \sigma_n^2}$$

$$\text{s.t.} \quad \theta^H \mathbf{F} \theta \le (1 - \beta) P_{\max} \tag{48}$$

where for briefly, we define

$$\mathbf{D} = \mathrm{diag}(\mathbf{f}^H)\mathbf{G}\mathbf{v}\mathbf{v}^H\mathbf{G}^H\,\mathrm{diag}(\mathbf{f}^H)^H,$$

$$\mathbf{t}^H = \mathbf{h}^H\mathbf{v}\mathbf{v}^H\mathbf{G}^H\,\mathrm{diag}(\mathbf{f}^H)^H,$$

$$\mathbf{E} = \sigma_1^2\,\mathrm{diag}(\mathbf{f}^H)\,\mathrm{diag}(\mathbf{f}^H)^H, \tag{49}$$

$$\mathbf{F} = \beta P_{\max}\,\mathrm{diag}(\mathbf{G}\mathbf{v})\,\mathrm{diag}(\mathbf{G}\mathbf{v})^H + \sigma_I^2\mathbf{I}_N.$$

Since this is a fractional programming problem, we can use the Dinkelbach's transform, then the optimization problem turns into

$$(\text{P3-1}) : \max_{\boldsymbol{\theta}} \quad \boldsymbol{\theta}^H\mathbf{D}\boldsymbol{\theta} + 2\Re\{\mathbf{t}^H\boldsymbol{\theta}\} - \eta(\boldsymbol{\theta}^H\mathbf{E}\boldsymbol{\theta} + \sigma_n^2)$$

$$\text{s.t.} \quad \boldsymbol{\theta}^H\mathbf{F}\boldsymbol{\theta} \le (1-\beta)P_{\max} \tag{50}$$

where η is an auxiliary variable, during each iteration process

$$\eta^{(i+1)} = \frac{\boldsymbol{\theta}^{(i)H}\mathbf{D}\boldsymbol{\theta}^{(i)} + 2\Re\{\mathbf{t}^H\boldsymbol{\theta}^{(i)}\}}{\boldsymbol{\theta}^{(i)H}\mathbf{E}\boldsymbol{\theta}^{(i)} + \sigma_n^2}. \tag{51}$$

Similarly, by using the first-order Taylor series expansion at fixed point $\boldsymbol{\theta}_0$, we have

$$\boldsymbol{\theta}^H\mathbf{D}\boldsymbol{\theta} \ge 2\Re\{\boldsymbol{\theta}_0^H\mathbf{D}\boldsymbol{\theta}\} - \boldsymbol{\theta}_0^H\mathbf{D}\boldsymbol{\theta}_0, \tag{52}$$

then, problem (P3-1) can be transformed into

$$(\text{P3-2}) : \max_{\boldsymbol{\theta}} \quad 2\Re\{\boldsymbol{\theta}_0^H\mathbf{D}\boldsymbol{\theta}\} + 2\Re\{\mathbf{t}^H\boldsymbol{\theta}\} - \eta(\boldsymbol{\theta}^H\mathbf{E}\boldsymbol{\theta} + \sigma_n^2)$$

$$\text{s.t.} \quad \boldsymbol{\theta}^H\mathbf{F}\boldsymbol{\theta} \le (1-\beta)P_{\max}. \tag{53}$$

The optimization problem (53) is convex, and we can address it by CVX directly. The process of algorithm to optimize $\boldsymbol{\Theta}$ is as follows:

Algorithm 1. The algorithm to optimize $\boldsymbol{\Theta}$.

1: Input $\mathbf{D}, \mathbf{t}^H, \mathbf{E}, \mathbf{F}$, initial value $\boldsymbol{\theta}^{(0)}, \eta^{(0)}, i = 0$, and convergence accuracy ξ.
repeat
    2: $i = i + 1$.
    3: Update $\eta^{(i)}, \eta^{(i)} = \frac{\boldsymbol{\theta}^{((i-1))H}\mathbf{D}\boldsymbol{\theta}^{(i-1)} + 2\Re\{\mathbf{t}^H\boldsymbol{\theta}^{(i-1)}\}}{\boldsymbol{\theta}^{((i-1))H}\mathbf{E}\boldsymbol{\theta}^{(i-1)} + \sigma_n^2}$.
    4: Let $\boldsymbol{\theta}_0 = \boldsymbol{\theta}^{(i-1)}$, solved problem (53) to obtain $\boldsymbol{\theta}^{(i)}$.
until $\boldsymbol{\theta}^{(i)H}\mathbf{D}\boldsymbol{\theta}^{(i)} + 2\Re\{\mathbf{t}^H\boldsymbol{\theta}^{(i)}\} - \eta^{(i)}(\boldsymbol{\theta}^{(i)H}\mathbf{E}\boldsymbol{\theta}^{(i)} + \sigma_n^2) \le \xi$.
5: Output $\boldsymbol{\theta}, \boldsymbol{\Theta} = \mathrm{diag}(\boldsymbol{\theta}^H)$.

3.4 Overall Strategy and Complexity Analysis

In this subsection, we have summarized the algorithm implementation of alternatingly optimizing variables β, $\boldsymbol{\Theta}$, and $\mathbf{v}$ as follows:

Due to the fact that the obtained solutions in Algorithm 2 are locally optimal, and the objective value sequence $\{\mathrm{AR}(\beta^{(k)}, \mathbf{v}^{(k)}, \boldsymbol{\Theta}^{(k)})\}$ obtained in each iteration of the alternate optimization method is non-decreasing. Specifically, it follows

$$\mathrm{AR}\left(\beta^{(k)}, \mathbf{v}^{(k)}, \boldsymbol{\Theta}^{(k)}\right)$$

$$\overset{(a)}{\le} \mathrm{AR}\left(\beta^{(k+1)}, \mathbf{v}^{(k)}, \boldsymbol{\Theta}^{(k)}\right)$$

$$\overset{(b)}{\le} \mathrm{AR}\left(\beta^{(k+1)}, \mathbf{v}^{(k+1)}, \boldsymbol{\Theta}^{(k)}\right) \tag{54}$$

$$\overset{(c)}{\le} \mathrm{AR}\left(\beta^{(k+1)}, \mathbf{v}^{(k+1)}, \boldsymbol{\Theta}^{(k+1)}\right)$$

where (a), (b), and (c) are due to the update in (30), (42), and (53), respectively. Moreover, $\mathrm{AR}\left(\beta^{(k)}, \mathbf{v}^{(k)}, \boldsymbol{\Theta}^{(k)}\right)$ has a finite upper bound since the limited power constraint. Therefore, the convergence of proposed Max-SNR-PA algorithm can be guaranteed.

Algorithm 2. Proposed Max-SNR-PA algorithm.

1: Initialize feasible solutions $\beta^{(0)}, \mathbf{v}^{(0)}$, and $\boldsymbol{\Theta}^{(0)}$, calculate the achievable rate $\mathrm{AR}^{(0)}$ based on (6).
2: Set iteration number $k = 0$, convergence accuracy ε.
repeat
    3: Given $\boldsymbol{\Theta}^{(k)}$ and $\mathbf{v}^{(k)}$ to obtain $\beta^{(k+1)}$ based on (30).
    4: Given $\boldsymbol{\Theta}^{(k)}$ and $\beta^{(k+1)}$ to obtain $\mathbf{v}^{(k+1)}$ based on (42).
    5: Given $\mathbf{v}^{(k+1)}$ and $\beta^{(k+1)}$ to obtain $\boldsymbol{\Theta}^{(k+1)}$ based on (53).
    6: $k = k + 1$.
until $|\mathrm{AR}^{(k)} - \mathrm{AR}^{(k-1)}| \le \varepsilon$.
7: $\mathbf{v}^{(k)}, \beta^{(k)}$, and $\boldsymbol{\Theta}^{(k)}$ are the optimal value, and $\mathrm{AR}^{(k)}$ is the optimal achievable rate.

The computational complexity of Algorithm 2 is mainly determined by the updates of the three variables β, $\mathbf{v}$, and $\boldsymbol{\Theta}$ via (30), (42), and (53), respectively. Specifically, the computational complexity of updating β is $O\left\{(Q+1)^4\right\}$ float-point operations (FLOPs). The complexity of updating $\mathbf{v}$ is $O\left\{6M^3\log_2(1/\varepsilon)\right\}$ FLOPs. The complexity of updating $\boldsymbol{\Theta}$ is $O\left\{\log_2(1/\varepsilon)L_{\boldsymbol{\Theta}}\log_2(1/\xi)\sqrt{N}(2N^4 + N^3)\right\}$ FLOPs. Thus, the overall computational complexity of Algorithm 2 is given by $O\left\{L_p[Q^4 + 6M^3\log_2(1/\varepsilon) + 2\log_2(1/\varepsilon)L_{\boldsymbol{\Theta}}\log_2(1/\xi)N^{4.5}]\right\}$, wherein Q is the order of fitting polynomial, ξ is the given accuracy tolerance of Algorithm 1, ε is the given accuracy tolerance of Algorithm 2, $L_{\boldsymbol{\Theta}}$ denotes the number of iterations required by Algorithm 1 for convergence, L_p denotes the number of iterations required by Algorithm 2 for convergence.

4. Proposed Max-AR-CFFP Strategy

In the previous section, we have proposed a PA strategy named Max-SNR-PA to achieve the power allocation between BS and active IRS. However, the computational complexity of this algorithm is too high. To address this issue, a low-complexity alternating iteration method will be presented as follows. This method differs by optimizing the beamforming vector of the BS and the active IRS phase shift matrix, with the optimization goal being the AR rather than the SNR. Thus, let us consider the system model hiding PA factor β mentioned in Sec. 2.2.

Our optimization goal is to maximize AR_1 by jointly optimizing $\mathbf{v}_1$ and $\boldsymbol{\Theta}$ under limited total power $P_{\max}$. The overall optimization problem is formulated as:

$$(P4) : \max_{\boldsymbol{\Theta}, \mathbf{v}_1} \quad AR_1$$

$$\text{s.t.} \quad P_{BS1} + P_{IRS1} \leq P_{\max}. \tag{55}$$

The joint design of $\boldsymbol{\Theta}$ and $\mathbf{v}_1$ is challenging due to the non-convexity and highly coupled variables in problem (P4). Therefore, in order to effectively solve this problem, we develop a joint beamforming and precoding scheme. By using the CFFP method in [33] Subsection III, introducing auxiliary variables γ and μ, equation (55) can be transformed as follows:

$$(P4\text{-}1) : \max_{\boldsymbol{\Theta}, \mathbf{v}_1, \gamma, \mu} \quad AR_1' = \ln(1 + \gamma) - |\mu|^2(\sigma_I^2 ||\mathbf{f}^H \boldsymbol{\Theta}||_2^2 + \sigma_n^2)$$
$$- \gamma + 2\sqrt{(1 + \gamma)} \Re\{\mu^*(\mathbf{f}^H \boldsymbol{\Theta} \mathbf{G} + \mathbf{h}^H)\mathbf{v}_1\}$$
$$\text{s.t.} \quad \mathbf{v}_1^H \mathbf{v}_1 + ||\boldsymbol{\Theta} \mathbf{G} \mathbf{v}_1||_2^2 + \sigma_I^2 ||\boldsymbol{\Theta}||_F^2 \leq P_{\max}. \tag{56}$$

Then, the locally optimal solution of (56) can be obtained by optimizing these variables alternately.

4.1 Optimize μ, given $\mathbf{v}_1$, $\boldsymbol{\Theta}$, and γ

After giving $\mathbf{v}_1$, $\boldsymbol{\Theta}$, and γ, the optimal μ can be obtained by solving $\frac{\partial AR_1'}{\partial \mu} = 0$ as

$$\mu^{opt} = \frac{\sqrt{(1 + \gamma)||(\mathbf{f}^H \boldsymbol{\Theta} \mathbf{G} + \mathbf{h}^H)\mathbf{v}_1||_2^2}}{\sigma_I^2 ||\mathbf{f}^H \boldsymbol{\Theta}||_2^2 + \sigma_n^2}. \tag{57}$$

4.2 Optimize γ, given $\mathbf{v}_1$, $\boldsymbol{\Theta}$, and μ

After giving $\mathbf{v}_1$, $\boldsymbol{\Theta}$, and μ, the optimal γ can be obtained by solving $\frac{\partial AR_1'}{\partial \gamma} = 0$ as

$$\gamma^{opt} = \frac{\varpi^2 + \varpi\sqrt{\varpi^2 + 4}}{2} \tag{58}$$

where $\varpi = \Re\{\mu^*(\mathbf{f}^H \boldsymbol{\Theta} \mathbf{G} + \mathbf{h}^H)\mathbf{v}_1\}$.

4.3 Optimize $\mathbf{v}_1$, given $\boldsymbol{\Theta}$, γ, and μ

For briefly, we define

$$\mathbf{H} = \mathbf{I}_M + \mathbf{G}^H \boldsymbol{\Theta}^H \boldsymbol{\Theta} \mathbf{G},$$
$$\mathbf{k}^H = 2\sqrt{(1 + \gamma)}\mu^*(\mathbf{f}^H \boldsymbol{\Theta} \mathbf{G} + \mathbf{h}^H), \tag{59}$$
$$P_r = P_{\max} - \sigma_I^2 ||\boldsymbol{\Theta}||_F^2$$

then, problem (P4-1) can be reformulated as follows

$$(P4\text{-}2) : \max_{\mathbf{v}_1} \quad \Re\{\mathbf{k}^H \mathbf{v}_1\}$$

$$\text{s.t.} \quad \mathbf{v}_1^H \mathbf{H} \mathbf{v}_1 \leq P_r. \tag{60}$$

This is a convex problem and it can be solved by CVX.

4.4 Optimize $\boldsymbol{\Theta}$, given $\mathbf{v}_1$, γ, and μ

Before solving this optimization problem, we have

$$\mathbf{f}^H \boldsymbol{\Theta} \mathbf{G} + \mathbf{h}^H = \boldsymbol{\theta}^H \text{diag}(\mathbf{f}^H)\mathbf{G} + \mathbf{h}^H,$$
$$||\boldsymbol{\Theta} \mathbf{G} \mathbf{v}_1||_2^2 = ||\boldsymbol{\theta}^H \text{diag}(\mathbf{G} \mathbf{v}_1)||_2^2, \tag{61}$$
$$||\boldsymbol{\Theta}||_F^2 = \boldsymbol{\theta}^H \boldsymbol{\theta}.$$

Utilizing (61), while giving $\mathbf{v}_1$, γ and μ, problem (P4-1) can be reformulated as

$$(P4\text{-}3) : \max_{\boldsymbol{\theta}} \quad \Re\{\boldsymbol{\theta}^H \mathbf{d}\} - \boldsymbol{\theta}^H \mathbf{J} \boldsymbol{\theta}$$

$$\text{s.t.} \quad \boldsymbol{\theta}^H \mathbf{L} \boldsymbol{\theta} \leq P_b \tag{62}$$

where

$$\mathbf{d} = 2\sqrt{(1 + \gamma)} \text{diag}(\mu^* \mathbf{f}^H)\mathbf{G} \mathbf{v}_1,$$
$$\mathbf{J} = |\mu|^2 \sigma_I^2 \text{diag}(\mathbf{f}^H) \text{diag}(\mathbf{f}^H)^H,$$
$$\mathbf{L} = \text{diag}(\mathbf{G} \mathbf{v}_1) \text{diag}(\mathbf{G} \mathbf{v}_1)^H + \sigma_I^2 \mathbf{I}_N, \tag{63}$$
$$P_b = P_{\max} - \mathbf{v}_1^H \mathbf{v}_1.$$

This is a convex problem, it could be solved by CVX. Then, we can obtain $\boldsymbol{\Theta} = \text{diag}(\boldsymbol{\theta}^H)$.

4.5 Overall Strategy and Complexity Analysis

In this subsection, we have summarized the algorithm implementation process for alternating optimization variables $\mathbf{v}_1$, $\boldsymbol{\Theta}$, μ, and γ as follows:

Algorithm 3. Proposed Max-AR-CFFP algorithm.

1: Initialize $\mathbf{v}_1^{(0)}, \boldsymbol{\Theta}^{(0)}, \mu^{(0)}$, and $\gamma^{(0)}$, calculate the signal-to-noise ratio $SNR_1^{(0)}$ and achievable rate $AR_1^{(0)}$ based on (11) and (12).
2: Set $t = 0$, convergence accuracy ζ.
repeat
  2: Update $\mu^{(t+1)}$ by (57).
  3: Update $\gamma^{(t+1)}$ by (58).
  4: Update $\mathbf{v}_1^{(t+1)}$ by (60).
  5: Update $\boldsymbol{\Theta}^{(t+1)}$ by (62).
  6: $t = t + 1$.
until $|AR_1^{(t)} - AR_1^{(t-1)}| \leq \zeta$.
7: $\mathbf{v}_1$ and $\boldsymbol{\Theta}$ are the optimal value, and AR_1 is the optimal achievable rate.

Algorithm 3 converges to a local optimum after multiple iterations, as the updates in each iteration step of the algorithm are the optimal solutions to the corresponding subproblems. Then, Algorithm 3 converges to

$$AR_1\left(\boldsymbol{\Theta}^{(t)}, \mathbf{v}_1^{(t)}, \gamma^{(t)}, \mu^{(t)}\right)$$
$$\overset{(d)}{\leq} AR_1\left(\boldsymbol{\Theta}^{(t)}, \mathbf{v}_1^{(t)}, \gamma^{(t)}, \mu^{(t+1)}\right)$$
$$\overset{(e)}{\leq} AR_1\left(\boldsymbol{\Theta}^{(t)}, \mathbf{v}_1^{(t)}, \gamma^{(t+1)}, \mu^{(t+1)}\right) \tag{64}$$
$$\overset{(f)}{\leq} AR_1\left(\boldsymbol{\Theta}^{(t)}, \mathbf{v}_1^{(t+1)}, \gamma^{(t+1)}, \mu^{(t+1)}\right)$$
$$\overset{(g)}{\leq} AR_1\left(\boldsymbol{\Theta}^{(t+1)}, \mathbf{v}_1^{(t+1)}, \gamma^{(t+1)}, \mu^{(t+1)}\right)$$

where (d), (e), (f), and (g) are due to the update in (57), (58), (60), and (62), respectively. Moreover, $\mathrm{AR}_1\left(\mathbf{\Theta}^{(t)}, \mathbf{v}_1^{(t)}, \gamma^{(t)}, \mu^{(t)}\right)$ has a finite upper bound since the limited power constraint. Therefore, we can guarantee the convergence of proposed Max-AR-CFFP algorithm.

The computational complexity of Algorithm 3 is mainly determined by the updates of the four variables μ, γ, $\mathbf{v}_1$, and $\mathbf{\Theta}$ via (57), (58), (60), and (62), respectively. The computational complexity of updating μ is $O\{N\}$ FLOPs. The computational complexity of updating γ is $O\{M\}$ FLOPs. The complexity of updating $\mathbf{v}_1$ is $O\left\{\log_2(1/\delta)\sqrt{M}(2M^4 + M^3)\right\}$ FLOPs. The complexity of updating $\mathbf{\Theta}$ is $O\left\{\log_2(1/\delta)\sqrt{N}(2N^4 + N^3)\right\}$ FLOPs. Thus, the overall computational complexity of Algorithm 3 is $O\left\{L_c\log_2(1/\delta)(M^{4.5} + N^{4.5})\right\}$, wherein δ is the given accuracy tolerance of Algorithm 3, L_c denotes the number of iterations required by Algorithm 3 for convergence.

5. Simulation and Discussion

In this section, simulation results are presented to prove the performance of the proposed two alternating iteration methods. We employ a personal computer to do simulation, which is equipped with AMD Ryzen 5900X and NVIDIA RTX4070TI. Figures are plotted by MATLAB. Unless otherwise specified in the discussion, the parameters are set as follows. The locations of BS, active IRS, and user are set to $(0\,\mathrm{m}, 30\,\mathrm{m}, 0\,\mathrm{m})$, $(50\,\mathrm{m}, 0\,\mathrm{m}, 10\,\mathrm{m})$, and $(25\,\mathrm{m}, 30\,\mathrm{m}, 0\,\mathrm{m})$, respectively. By using the path loss model in [15], the large-scale path loss in dB is $\mathrm{PL} = \mathrm{PL}_0 - 10\alpha\log_{10}\left(\frac{d}{d_0}\right)$, where PL_0 is the path-loss at the reference distance d_0, d is the link distance, α is the path-loss exponent. We set $\mathrm{PL}_0 = -30\,\mathrm{dB}$ and $d_0 = 1\,\mathrm{m}$. Following [14], the randomly generated channel matrix $\mathbf{G}$, channel vectors $\mathbf{f}$, and $\mathbf{h}$ follow the Rayleigh distribution. The number of BS antennas is chosen as follows: $M = 2$, noise power $\sigma_\mathrm{I}^2 = \sigma_n^2 = -100\,\mathrm{dBm}$. We use the random number generation function rand() in MATLAB, the simulation parameters in two proposed algorithms are set to $\beta^{(0)} = 0.5$, $\mathbf{v}^{(0)} = \mathrm{e}^{\mathrm{j}2\cdot\pi\cdot\mathrm{rand}(N,1)}/|\mathrm{e}^{\mathrm{j}2\cdot\pi\cdot\mathrm{rand}(N,1)}|$, $\mathbf{\Theta}^{(0)} = \mathrm{diag}\left(\mathrm{e}^{\mathrm{j}2\cdot\pi\cdot\mathrm{rand}(N,1)}\right)$ and $\mathbf{v}_1^{(0)} = \mathrm{e}^{\mathrm{j}2\cdot\pi\cdot\mathrm{rand}(N,1)}$, $\mathbf{\Theta}^{(0)} = \mathrm{diag}\left(\mathrm{e}^{\mathrm{j}2\cdot\pi\cdot\mathrm{rand}(N,1)}\right)$, $\gamma^{(0)} = \mathrm{SNR}_1^{(0)}$.

Figure 2 illustrates the curves of rate expression and its polynomial regression rate expression versus the PA factor β for four distinct cases: $J = 201, Q = 3$; $J = 101, Q = 3$; $J = 201, Q = 2$; and $J = 101, Q = 2$ with $N = 128$ and $P_\mathrm{max} = 30\,\mathrm{dBm}$. Channel path fading factors from BS to IRS, IRS to user, and BS to user are set to $\alpha_\mathrm{BI} = 2.1$, $\alpha_\mathrm{IU} = 2.1$, $\alpha_\mathrm{BU} = 4.0$, respectively. From Fig. 2, it can be seen that all four cases can fit the original rate curve well. As the number of sampling points J and fitting order Q increase, the polynomial regression fitting improves.

Figure 3 illustrates the convergence behaviour of the proposed Max-SNR-PA method for two distinct active IRS

phase shift elements: $N = 32$ and $N = 128$ with $P_\mathrm{max} = 30\,\mathrm{dBm}$, $\alpha_\mathrm{BI} = 2.1$, $\alpha_\mathrm{IU} = 2.1$, $\alpha_\mathrm{BU} = 4.0$. From Fig. 3, it is seen that the AR of proposed method increase rapidly with the number of iterations and finally converge to a value after a finite number of iterations. As J and Q increase, the AR performance of the proposed methods can be gradually improved. Considering that the rate difference between two cases: $J = 201, Q = 3$ and $J = 101, Q = 3$ is less than 0.2 bit, the number of sampling points J and fitting order Q are chosen to be 201 and 3.

Figure 4 shows the convergence behaviour of the two proposed methods for two different active IRS phase-shifting elements: $N = 32$ and $N = 128$. Here, $P_\mathrm{max} = 30\,\mathrm{dBm}$, $\alpha_\mathrm{BI} = 2.1$, $\alpha_\mathrm{IU} = 2.1$, $\alpha_\mathrm{BU} = 4.0$. From Fig. 4, it is shown that as the number of iterations increases, the proposed Max-AR-CFFP method can also achieve convergence. But the convergence speed of Max-AR-CFFP method is slower than that of Max-SNR-PA method.
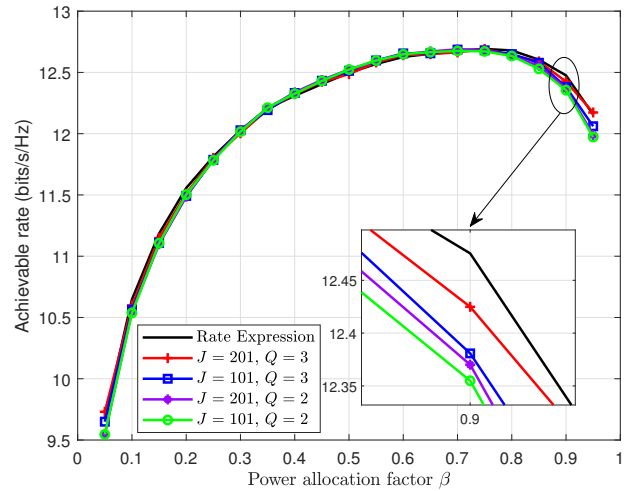
Fig. 2. Achievable rate versus PA factor β.
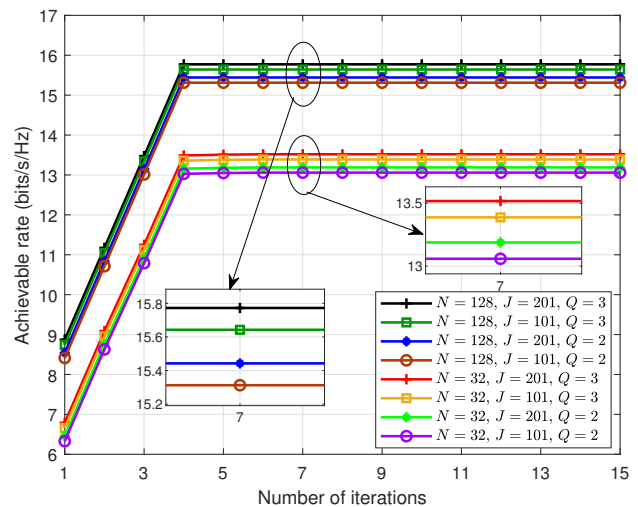
Fig. 3. Convergence behaviour of the proposed Max-SNR-PA method.
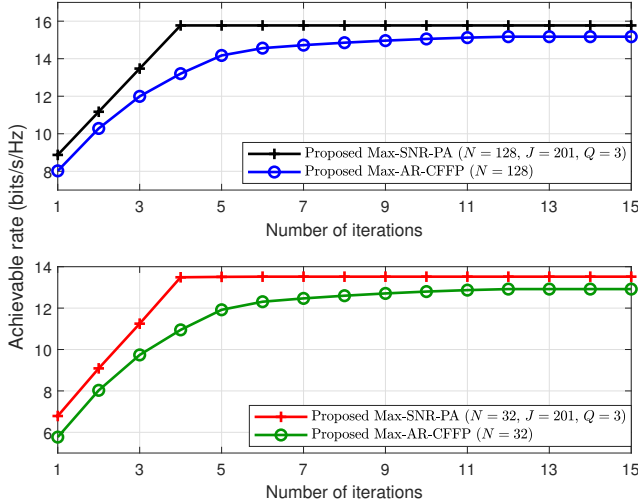
Fig. 4. Convergence behaviour of the proposed two method.

Figures 5–7 plot the achievable rates of the proposed Max-SNR-PA and Max-AR-CFFP methods versus the number of active IRS elements N with fixed PA factor $\beta = 0.8$, fixed PA factor $\beta = 0.99$ [35], fixed PA factor $\beta = 0.5$, GA method [36], passive IRS, random phase shift, and without IRS as performance benchmarks. Here, $P_{max} = 30$ dBm, $\alpha_{BI} = 2.1$, $\alpha_{IU} = 2.1$. The channel path fading factor from BS to user in Figs. 5, 6, 7 are set to $\alpha_{BU} = 4.0$, $\alpha_{BU} = 3.0$, and $\alpha_{BU} = 2.1$, respectively. This means that the direct link strength from BS to user are weak, medium and strong, respectively.

From these three figures, we can see that as the number of IRS elements N increases, the rates of all nine methods will be promoted. The proposed two methods can achieve an obvious rate performance gains over fixed PA factor $\beta = 0.8$, $\beta = 0.99$, $\beta = 0.5$, GA method, passive IRS, random phase shift, and without IRS. Especially, with the enhancement of direct link between BS and user, the improvement effect of passive IRS on rate performance gradually deteriorates, and the two proposed PA strategies can still effectively improve rate performance.

Figures 8–10 illustrate the curves of achievable rate versus total transmit power P_{max}, where $N = 128$, $\alpha_{BI} = 2.1$, $\alpha_{IU} = 2.1$. Here, α_{BU} are set to 4.0, 3.0, and 2.1 in Figs. 8, 9, 10, respectively. These three figures are shown that as P_{max} increases, all nine curves in figures has an upward trend. When the direct link between BS and user is gradually enhanced, the proportion of signal strength transmitted through direct link in user received signals will be gradually improved. Thus, the rate performance advantages of two proposed PA strategies are more prominent in the cases of weak direct link and medium strength direct link. In summary, nine methods have an increasing order in rate performance as follows: Max-SNR-PA, Max-AR-CFFP, fixed PA factor $\beta = 0.8$, fixed PA factor $\beta = 0.99$ [35], fixed PA factor $\beta = 0.5$, GA method [36], passive IRS, random phase shift, and without IRS.
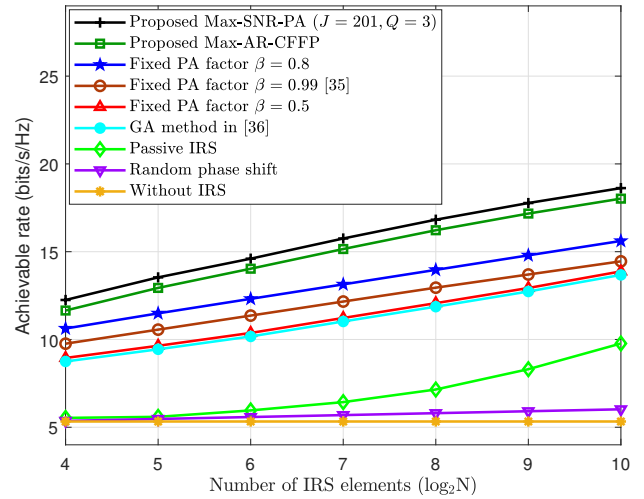
Fig. 5. Achievable rate versus the number of active IRS elements N with a weak direct link.
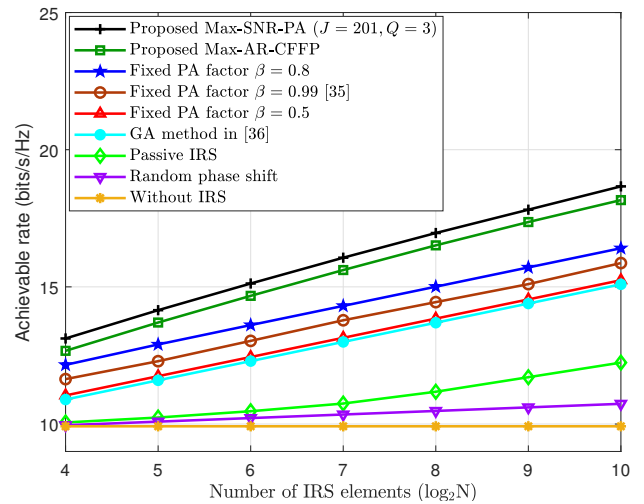
Fig. 6. Achievable rate versus the number of active IRS elements N with a medium strength direct link.
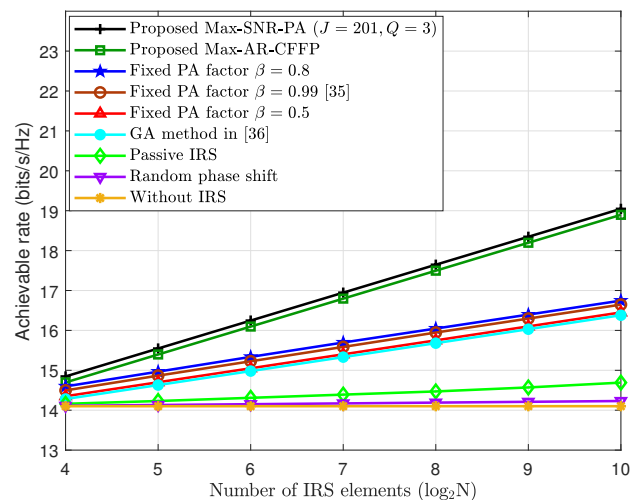
Fig. 7. Achievable rate versus the number of active IRS elements N with a strong direct link.
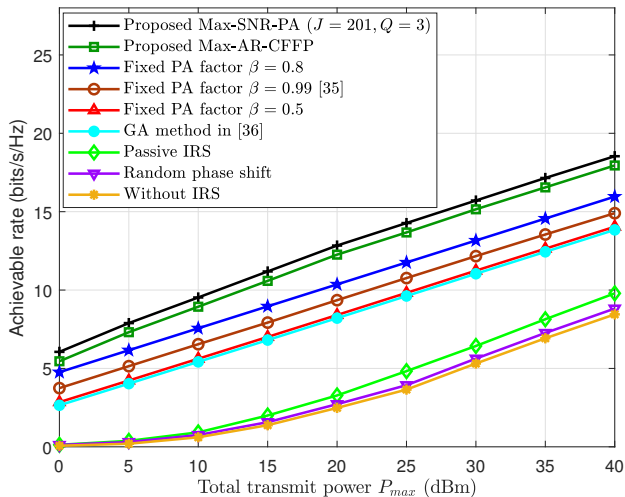
Fig. 8. Achievable rate versus total transmit power P_{max} with a weak direct link.
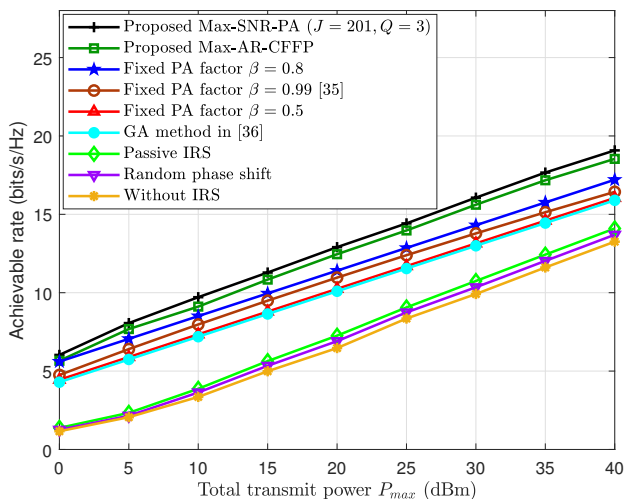
Fig. 9. Achievable rate versus total transmit power $P_{\max}$ with a medium strength direct link.
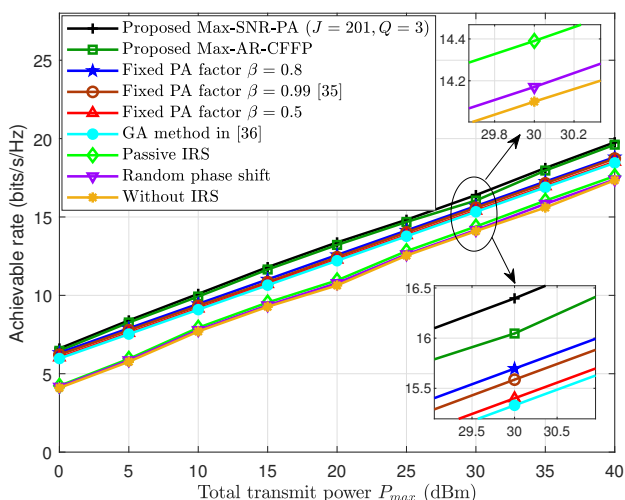
Fig. 10. Achievable rate versus total transmit power $P_{\max}$ with a strong direct link.

6. Conclusion

In this paper, we investigated the AR performance of an active IRS-aided wireless network with PA. To improve the AR performance, under a limited total power constraint, a SNR maximization problem was constructed by jointly optimizing PA factor, active IRS phase shift matrix, and BS beamforming vector. To address the non-convex problem, an alternating optimization method was used. Specifically, the PA factor was obtained by polynomial regression method, BS and IRS beamformings were derived based on Dinkelbach's transform and successive convex approximation techniques. To reduce the computational complexity of above proposed strategy, we maximize AR and alternately optimize BS and IRS beamformings by a closed-form fractional programming method. Simulation results proved that our proposed two strategies obviously outperform the benchmark schemes and can achieve significant AR performance gains. For future work, the PA strategies in multiple-input multiple-output wireless communication networks can be researched and analyzed.

Acknowledgments

References

[1] PAN, C., REN, H., WANG, K., et al. Reconfigurable intelligent surfaces for 6G systems: Principles, applications, and research directions. *IEEE Communications Magazine*, 2021, vol. 59, no. 6, p. 14–20. DOI: 10.1109/MCOM.001.2001076

[2] DENG, N., SHI, X., SHENG, M., et al. Enhancing millimeter wave cellular networks via UAV-borne aerial IRS swarms. *IEEE Transactions on Communications*, 2024, vol. 72, no. 1, p. 524–538. DOI: 10.1109/TCOMM.2023.3320701

[3] YANG, L., YANG, Y., HASNA, M. O., et al. Coverage, probability of SNR gain, and DOR analysis of RIS-aided communication systems. *IEEE Wireless Communications Letters*, 2020, vol. 9, no. 8, p. 1268–1272. DOI: 10.1109/LWC.2020.2987798

[4] SHU, F., WU, X., HU, J., et al. Secure and precise wireless transmission for random-subcarrier-selection-based directional modulation transmit antenna array. *IEEE Journal on Selected Areas in Communications*, 2018, vol. 36, no. 4, p. 890–904. DOI: 10.1109/JSAC.2018.2824231

[5] WANG, W., ZHANG, W. Joint beam training and positioning for intelligent reflecting surfaces assisted millimeter wave communications. *IEEE Transactions on Wireless Communications*, 2021, vol. 20, no. 10, p. 6282–6297. DOI: 10.1109/TWC.2021.3073140

[6] SHU, F., QIN, Y., LIU, T., et al. Low-complexity and high-resolution DOA estimation for hybrid analog and digital massive MIMO receive array. *IEEE Transactions on Communications*, 2018, vol. 66, no. 6, p. 2487–2501. DOI: 10.1109/TCOMM.2018.2805803

[7] WU, Q., ZHANG, R. Beamforming optimization for wireless network aided by intelligent reflecting surface with discrete phase shifts. *IEEE Transactions on Communications*, 2020, vol. 68, no. 3, p. 1838–1851. DOI: 10.1109/TCOMM.2019.2958916

[8] LIU, R., WU, Q., RENZO, D. M., et al. A path to smart radio environments: An industrial viewpoint on reconfigurable intelligent surfaces. *IEEE Wireless Communications*, 2022, vol. 29, no. 1, p. 202–208. DOI: 10.1109/MWC.111.2100258

[9] SHI, W., WU, Q., WU, D., et al. Joint transmit and reflective beamforming design for active IRS-aided SWIPT systems. *Chinese Journal of Electronics*, 2024, vol. 33, no. 2, p. 536–548. DOI: 10.23919/cje.2022.00.287

[10] MUHAMMAD, H. A., FAISAL, A., IMRAN, R., et al. Pilots optimization and surface area effects on channel estimation in RIS aided MIMO system. *Radioengineering*, 2023, vol. 32, no. 2, p. 187–196. DOI: 10.13164/re.2023.0187

[11] WU, Q., ZHANG, R. Intelligent reflecting surface enhanced wireless network via joint active and passive beamforming. *IEEE Transactions on Wireless Communications*, 2019, vol. 18, no. 11, p. 5394–5409. DOI: 10.1109/TWC.2019.2936025

[12] HUANG, C., MO, R., YUEN, C. Reconfigurable intelligent surface assisted multiuser MISO systems exploiting deep reinforcement learning. *IEEE Journal on Selected Areas in Communications*, 2020, vol. 38, no. 8, p. 1839–1850. DOI: 10.1109/JSAC.2020.3000835

[13] SHI, W., WU, Q., XIAO, F., et al. Secrecy throughput maximization for IRS-aided MIMO wireless powered communication networks. *IEEE Transactions on Communications*, 2022, vol. 70, no. 11, p. 7520–7535. DOI: 10.1109/TCOMM.2022.3212734

[14] PAN, C., REN, H., WANG, K., et al. Multicell MIMO communications relying on intelligent reflecting surfaces. *IEEE Transactions on Wireless Communications*, 2020, vol. 19, no. 8, p. 5218–5233. DOI: 10.1109/TWC.2020.2990766

[15] LIN, Y., SHU, F., DONG, R., et al. Enhanced-rate iterative beamformers for active IRS-assisted wireless communications. *IEEE Wireless Communications Letters*, 2023, vol. 12, no. 9, p. 1538–1542. DOI: 10.1109/LWC.2023.3281821

[16] ZHAO, W., WANG, G., ATAPATTU, S., et al. Is backscatter link stronger than direct link in reconfigurable intelligent surface-assisted system? *IEEE Communications Letters*, 2020, vol. 24, no. 6, p. 1342–1346. DOI: 10.1109/LCOMM.2020.2980510

[17] LV, W., BAI, J., YAN, Q., et al. RIS-assisted green secure communications: Active RIS or passive RIS? *IEEE Wireless Communications Letters*, 2023, vol. 12, no. 2, p. 237–241. DOI: 10.1109/LWC.2022.3221609

[18] LI, Y., YOU, C., CHUN, Y. J., et al. Active-IRS aided wireless network: System modeling and performance analysis. *IEEE Communications Letters*, 2023, vol. 27, no. 2, p. 487–491. DOI: 10.1109/LCOMM.2022.3221116

[19] YANG, X., WANG, H., FENG, Y. Sum rate maximization for active RIS-aided uplink multi-antenna NOMA systems. *IEEE Wireless Communications Letters*, 2023, vol. 12, no. 7, p. 1149–1153. DOI: 10.1109/LWC.2023.3264516

[20] LI, X., YOU, C., KANG, Z., et al. Double-active-IRS aided wireless communication with total amplification power constraint. *IEEE Communications Letters*, 2023, vol. 27, no. 10, p. 2817–2821. DOI: 10.1109/LCOMM.2023.3298070

[21] ZHI, K., PAN, C., REN, H., et al. Active RIS versus passive RIS: Which is superior with the same power budget? *IEEE Communications Letters*, 2022, vol. 26, no. 5, p. 1150–1154. DOI: 10.1109/LCOMM.2022.3159525

[22] SHU, F., LIU, J., LIN, Y., et al. Three high-rate beamforming methods for active IRS-aided wireless network. *IEEE Transactions on Vehicular Technology*, 2023, vol. 72, no. 11, p. 15052–15056. DOI: 10.1109/TVT.2023.3279840

[23] ZHU, Q., LI, M., LIU, R., et al. Joint beamforming designs for active reconfigurable intelligent surface: A sub-connected array architecture. *IEEE Transactions on Communications*, 2022, vol. 70, no. 11, p. 7628–7643. DOI: 10.1109/TCOMM.2022.3212749

[24] KANG, J., KIM, I., KIM, D. Joint TX power allocation and RX power splitting for SWIPT system with multiple nonlinear energy harvesting circuits. *IEEE Wireless Communications Letters*, 2019, vol. 8, no. 1, p. 53–56. DOI: 10.1109/LWC.2018.2851229

[25] LIU, H., ZHU, P., CHEN, Y., et al. Power allocation for downlink hybrid power line and visible light communication system. *IEEE Access*, 2020, vol. 8, p. 24145–24152. DOI: 10.1109/ACCESS.2020.2970097

[26] LEE, H., MODIANO, E., LE, L. Distributed throughput maximization in wireless networks via random power allocation. *IEEE Transactions on Mobile Computing*, 2012, vol. 11, no. 4, p. 577–590. DOI: 10.1109/TMC.2011.58

[27] LU, W., GONG, Y., WU, J., et al. Simultaneous wireless information and power transfer based on joint subcarrier and power allocation in OFDM systems. *IEEE Access*, 2017, vol. 5, p. 2763–2770. DOI: 10.1109/ACCESS.2017.2671903

[28] WAN, S., SHU, F., LU, J., et al. Power allocation strategy of maximizing secrecy rate for secure directional modulation networks. *IEEE Access*, 2018, vol. 6, p. 38794–38801. DOI: 10.1109/ACCESS.2018.2815779

[29] SHU, F., LIU, X., XIA, G., et al. High-performance power allocation strategies for secure spatial modulation. *IEEE Transactions on Vehicular Technology*, 2019, vol. 68, no. 5, p. 5164–5168. DOI: 10.1109/TVT.2019.2905765

[30] HUANG, X., ANSARI, N. Joint spectrum and power allocation for multi-node cooperative wireless systems. *IEEE Transactions on Mobile Computing*, 2015, vol. 14, no. 10, p. 2034–2044. DOI: 10.1109/TMC.2015.2388478

[31] CHEN, L., HAN, S., MENG, W., et al. Power allocation for single-stream dual-hop full-duplex decode-and-forward MIMO relay. *IEEE Communications Letters*, 2016, vol. 20, no. 4, p. 740–743. DOI: 10.1109/LCOMM.2016.2525777

[32] SUN, Y., BABU, P., PALOMAR, D. Majorization-minimization algorithms in signal processing, communications, and machine learning. *IEEE Transactions on Signal Processing*, 2017, vol. 65, no. 3, p. 794–815. DOI: 10.1109/TSP.2016.2601299

[33] SHEN, K., YU, W. Fractional programming for communication systems–Part I: Power control and beamforming. *IEEE Transactions on Signal Processing*, 2018, vol. 66, no. 10, p. 2616–2630. DOI: 10.1109/TSP.2018.2812733

[34] SHEN, K., YU, W. Fractional programming for communication systems–Part II: Uplink scheduling via matching. *IEEE Transactions on Signal Processing*, 2018, vol. 66, no. 10, p. 2631–2644. DOI: 10.1109/TSP.2018.2812748

[35] ZHANG, Z., DAI, L., CHEN, X., et al. Active RIS vs. passive RIS: Which will prevail in 6G? *IEEE Transactions on Communications*, 2023, vol. 71, no. 3, p. 1707–1725. DOI: 10.1109/TCOMM.2022.3231893

[36] ZHAO, Y., WANG, X., WANG, Y., et al. High-performance power allocation strategies for active IRS-aided wireless network. *arXiv*, 2023, p. 1–5. DOI: 10.48550/arXiv.2311.04032

[37] BISHOP, C. M. *Pattern Recognition and Machine Learning*. 1st ed., rev. New York (USA): Springer, 2007. ISBN: 9780387310732

About the Authors . . .

Qiankun CHENG received the B.E. degree from Anhui Normal University, China, in 2022. He is currently pursuing the M.S. degree with the School of Information and Communication Engineering, Hainan University, China. His research interests include intelligent reflecting surface and machine learning.

Jiatong BAI is currently pursuing the Ph.D. degree with the School of Information and Communication Engineering, Hainan University, China. Her research interests include wireless communication and machine learning.

Xuehui WANG received the M.S. degree from Hainan University, China, in 2020, where she is currently pursuing the Ph.D. degree with the School of Information and Communication Engineering. Her research interests include wireless communication, signal processing, and IRS-aided relay systems.

Baihua SHI is currently pursuing the Ph.D. degree with the School of Electronic and Optical Engineering, Nanjing University of Science and Technology, China. His research interests include wireless communication and signal processing.

Wei GAO (corresponding author) received the B.E. degree in Communication Engineering and the Ph.D. degree of Information and Communication Engineering from the Huazhong University of Science and Technology (HUST) in 2014 and 2020, respectively. He is currently a postdoc with Hainan University. His research interests include network architecture, wireless network access and radio resources allocation.

Feng SHU was born in 1973. He received the B.S. degree from Fuyang Teaching College, Fuyang, China, in 1994, the M.S. degree from Xidian University, Xian, China, in 1997, and the Ph.D. degree from Southeast University, Nanjing, China, in 2002. From 2009 to 2010, he was a Visiting Postdoctoral Fellow with the University of Texas at Dallas, Richardson, TX, USA. From July 2007 to September 2007, he was a Visiting Scholar with the Royal Melbourne Institute of Technology, Melbourne VIC, Australia. From 2005 to 2020, he was with the School of Electronic and Optical Engineering, Nanjing University of Science and Technology, Nanjing, where he was promoted from an Associate Professor to a Full Professor of supervising Ph.D. students in 2013. Since 2020, he has been with the School of Information and Communication Engineering, Hainan University, Haikou, China, where he is currently a Professor and a Supervisor of Ph.D. and graduate students. He has authored or coauthored more than 300 in archival journals with more than 150 papers on IEEE journals and 250 SCI-indexed papers. His research interests include wireless networks, wireless location, and array signal processing. He was awarded with the Leading-Talent Plan of Hainan Province in 2020, the Fujian Hundred-Talent Plan of Fujian Province in 2018, and the Mingjian Scholar Chair Professor in 2015. His citations are more than 8000 times. He holds one US patent and more than 40 Chinese patents. He is also a PI or CoPI for eight national projects. He was an Exemplary Reviewer for IEEE Transactions on Communications in 2020. He is currently the Editor of IEEE Wireless Communications Letters and guest editor for the Chinese Journal of Aeronautics and Journal of Electronics Information Technology. He was the Editor of IEEE Systems Journal from 2019 to 2021 and IEEE Access from 2016 to 2018 and also guest editor for IET Communications and Security and Safety etc.